

# A Transcranial Magnetic Stimulation Coil Using Rectangular Braided *Litz* Wire

Mehran Talebinejad, and Sam Musallam

Department of Electrical and Computer Engineering, and  
Department of Physiology, McGill University  
Montreal, Quebec, CANADA  
mehran.talebinejad@mcgill.ca

Andrew E. Marble

Department of Systems and Computer Engineering  
Carleton University  
Ottawa, Ontario, CANADA

**Abstract**—A transcranial magnetic stimulation coil built by rectangular braided *Litz* wire is presented. The rectangular braided *Litz* wire used in this work is comprised of 2500 ultrafine wires, rated for high currents and voltages necessary for magnetic stimulation (10 kA, and 3 kV). The wire is only 7.3 mm wide and 0.9 mm thick making it amenable to tighter windings yielding high magnetic fields with a small coil diameter, and reduces coil heating issues. The coil is 3.1 cm in diameter and provides a magnetic field higher than the smallest available commercial coil despite being 40% smaller. This potentially expands research and therapeutic functionalities of transcranial magnetic stimulation, especially increases the stimulation specificity for use in neural prosthetic systems and bidirectional brain machine interfaces.

**Keywords**—component; bioelectric potentials; biomagnetics; neural stimulation; transcranial magnetic stimulation coil; braided *Litz* wire;

## I. INTRODUCTION

Transcranial magnetic stimulation (TMS) is a well established tool for noninvasive stimulation of neural tissues [1-6]. Generally, a sine pulsed current is injected into the TMS coil from a discharge capacitor which results in a magnetic field that induces a damped cosine electric field in the neural tissue and leads to neural activation [4-8]. Excitatory and inhibitory characteristics of TMS have been used in a wide spectrum of research and therapeutic applications [8-11].

Recent advances in high voltage DC-DC convertor, IGBT, and capacitor technology [12-15] has improved TMS instrumentation by allowing adjustable amplitude, duration, number and polarity of the pulsed current [12-15]. However, the stimulated area is primarily dictated by the coil's geometry. Most of the previous research on TMS coil is based on mathematical optimization of the focality [16-20] and has not been realized due to practical limitations. Despite the introduction of several complex TMS coil models, a single circular coil is still the most focal available in practice [1-6].

In this paper, we present a TMS coil built by rectangular braided *Litz* wire comprised of 2500 ultrafine wires. We demonstrate that this coil is capable of producing a magnetic field sufficient for TMS and as high as available commercial coils, but with the advantage of being 40 % smaller than the smallest available TMS coil. Potential improvements of

heating issues, acoustic noise and future applications are also discussed.

## II. METHODS AND MATERIALS

### A. Rectangular Braided *Litz* wire

In previous work, we showed that rectangular wire outperforms round and square wires in the context of TMS coil [21]. The rectangular wire can create coils with tighter windings which result in a greater magnetic field compared to round and square wires with the same coil diameter. However, rectangular single conductor wires are limited in thickness due to practical issues of wire fabrication. Also, the conductivity in rectangular single conductor wires is significantly reduced by skin effects, leading to excessive power dissipation and heating issues [21]. These limitations and shortcomings have led to more elaborate wire designs with multiple conductors [22-23]. A *Litz* wire is comprised of several conductors that are individually insulated. The resultant isolation between the wires effectively removes the skin effect, and significantly reduces undesirable induced currents and heating issues [21-23].

The rectangular *Litz* wire described in [21] was fabricated through standard wire processes. This wire is comprised of 2500 ultrafine,  $2 \mu\text{m}^2$  round wires (minimum number required for 10 kA and 3 kV) that are braided to form a rectangular cross section. This wire is 7.1 mm wide and 0.7 mm in thickness. Each ultrafine wire is insulated with enamel film and the wires are braided in a *Litz* configuration [22-23]. To avoid shorts due to incomplete enamel coverage, the wire is also insulated by an ETFE layer which adds an additional  $2 \times 0.1$  mm to the width and thickness. The ETFE layer also protects the ultrafine wires and keeps the rectangular cross section. This wire shown in Fig. 1 is the basis of coil design in this work.

The ETFE layer and enamel film must be stripped for electrical connection of the braided *Litz* wire. To avoid damaging the ultrafine wires, the ETFE layer was removed using a rectangular wire stripper (Eraser L2SA). The enamel film was removed using *Corrosive Caustic Soda* melted in a hot pot (Eraser DSP1) at 400 °C and then the wire was cleaned and neutralized using *Ammonium Chloride* and *Citric Acid* [24].

## B. Coil design

Based on the fabricated wire dimensions, a suitable coil design was explored. We implement the coils as a horizontal-spiral winding as this geometry outperforms the vertical-spiral winding when a rectangular wire is used for TMS coil [21].

The inner diameter and outer diameter define the geometry of a horizontal-spiral coil. The inner diameter can be as small as the wire's width which is dictated by the winding apparatus pulley. In this work, given the 7.3 mm wire width, an 8 mm pulley was used which was the closest available dimension. The outer diameter also determines the number of turns and the strength of the magnetic field as well as the stimulation specificity. The smallest outer diameter was shown to provide a magnetic field with sufficient strength for TMS [21]. A TMS coil must be capable of producing a 1.8 to 3 Tesla magnetic field with a rise time between 50 to 100  $\mu$ s, given 8 to 10 kA coil current [1-2]. These values are enough to induce a 10 to 20 mA/cm<sup>2</sup> current density leading to a 30 to 40 mV neuronal membrane depolarization [1-2]. Below, we describe finite element simulations to determine the outer diameter that can generate the required fields.

## C. Finite Element Simulation

The COMSOL Multiphysics, 3D AC/DC Module 3.4, was employed for finite element simulations.

The stimulator circuit was approximated as a 10 kA constant current source for steady state analysis [21].

The coil was first designed with 3D specification in AUTOCAD and then imported to the AC/DC Module for finite element simulations. The number of turns in the coil was then varied until the minimum requirements of the magnetic field were satisfied empirically. Inductance and resistance of the coil were automatically measured and updated based on the physical characteristics of the specified material and coil geometry (wire length). Current density in the coil was computed azimuthally as,

$$J_{\phi} = \nabla \times (\mu^{-1} \nabla \times A_{\phi}), \quad (1)$$

where  $\mu$  is the relative permeability (copper = air = 1) and  $A_{\phi}$  is the magnetic vector potential. Using Eq 1, the Magnetic field magnitude was computed on a uniform 0.01 mm triangle mesh using the finite element method. The goal of the simulation was to find the minimum outer diameter dictated by the necessary minimum number of turns that yields a field of 3 Tesla. The minimum number of turns was found empirically to be 12, which gives a coil with 3.1 cm outer diameter named MT1.

After determining the necessary dimensions with simulations the coil prototype was wound and validated in an experimental setup described in the next section.

## D. Experimental Setup

Four coils were compared: 1) one layer 3.1 cm coil MT1, 2) two MT1s in a two layer format named MT2, 3) MagStim 1924 coil which is 9 cm, and 4) MagStim D25BI which is 5 cm.

Available Gaussmeters are not capable of measuring the magnetic field of a coil generated by a pulsed current in a few  $\mu$ s. It is also not possible to prolong the duration of the pulse with a current of a few kA. To compare the coils, we measured the magnetic field surrounding the coil due to a small current in the steady state. The transient current and rise time of the first resonance are determined by the inductance and the capacitance of the coil and the discharge system respectively. Inductance of this coil is 15  $\mu$ H, close to commercial coils and the first resonance duration is shorter than 100  $\mu$ s. As the magnetic field is directly proportional to the current in the coil, results are readily scaled to realistic current values [25].

Each coil was connected to the current source (HP 6824A) which was adjusted so that a 1 A current runs through the coil, serially in case of the MagStim double coils and the two layer coil MT2. Meanwhile, the magnetic field surrounding each coil was measured using a 3-axis Gaussmeter (Lakeshore 460). The probe of the Gaussmeter was scanned over the surface of each coil using a Velmex 3-axis position stage. Field measurements were made every 2.5 mm. The magnitude of the recorded magnetic field is reported in this paper in Fig. 2, and Table I.

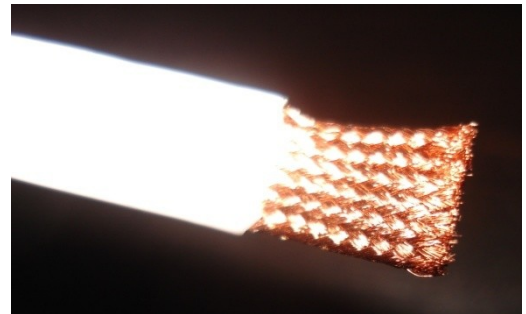


Figure 1. Braided Litz wire with ETFE insulation.

## III. RESULTS AND DISCUSSIONS

Fig. 2, shows the topographic map of the magnetic field surrounding each of the four coils. Table I, summarizes the maximum magnetic field and specifications of each coil.

In response to 1 A of current, the MagStim coils 1924 and D25BI produced a magnetic field with magnitudes of 2.400 and 2.470 Gauss respectively. These values are consistent with device's rated performance of 2.5 Tesla given 10 kA current. The MT1 and MT2 produce a magnetic field with magnitudes of 2.409 and 3.363 Gauss respectively; it is expected that they give 2.409 and 3.363 Tesla with 10 kA current which is consistent with the design criteria and finite element simulations. These results validate the functionality of the MT1 and MT2 prototypes for TMS. The greater magnetic field of the MT2 compared to the MT1 could be explained by the superposition of magnetic fields of two MT1s, which results into a greater overall magnetic field. Because layering preserves the specificity of the stimulation [21], this technique seems to be valuable. Indeed new versions of the MagStim coils (e.g., air film coils) employ more than one layer.

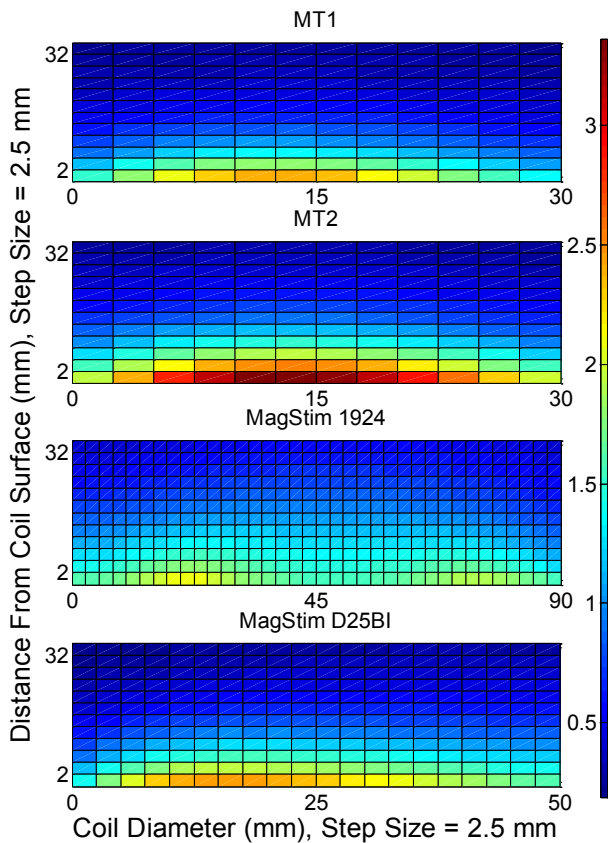


Figure 2. Magnetic field map of each coil in Gauss resulted from a 1 A current. The horizontal and vertical axes correspond to the coil diameter and top surface respectively. MT2 shows the darkest plot at the center of the coil corresponding to the maximum field strength 3.363 Gauss. The 1924 has the largest outer and inner diameter and center of the coil poses a lower magnetic field strength. Magnetic field of the D25BI is tilted to the left which is due to the coil's bending angle.

#### IV. CONCLUSIONS

MT2 provides a higher magnetic field compared to the 1924, and D25BI, despite being smaller. This confirms the suitability of the braided *Litz* wire for TMS coil applications and is consistent with previous works [21]. This potentially expands research and therapeutic functionalities of TMS. Further research is required to determine suitability of using this coil in conjunction with neural prosthetic systems and bidirectional brain machine interfaces.

In Future work, we will examine MT2 with an actual inductance matched stimulator to study the transitory current of this coil.

Preliminary results show the acoustic noise caused by the stimulation is lower when the braided *Litz* wire is used compared to a single conductor wire; this could be explained by higher flexibility of this wire.

Further work is also required to examine improvements of heating issues compared to the single conductor wires.

Simulation results [21] show the induced currents inside the wire are greatly reduced when the Braided *Litz* wire is used; this reduces the overall wire current and is expected to improve undesirable heating during prolonged rapid TMS.

TABLE I. SUMMARY OF COILS' SPECIFICATIONS

Coil type	MT1	MT2	1924	D26BI
Diameter (cm)	3.1	3.1	9	5
# of turns	12	12	6	6
# of layers	1	2	1	1
Max. magnetic field (Gauss)	2.409	3.363	2.400	2.470

#### REFERENCES

- [1] E.M. Wassermann; C. Epstein; U. Ziemann; V. Walsh; T. Paus; S.H. Lisanby; *Oxford Handbook of Transcranial Stimulation*. Oxford: Oxford University Press. pp. 13–23, 2008.
- [2] R. Simone; H. Mark; M.R. Paolo; P.L. Alvaro; , "Safety, ethical considerations, and application guidelines for the use of transcranial magnetic stimulation in clinical practice and research," *Clinical Neurophysiology*, vol.120, no.12, pp.2008-2039, 2009.
- [3] P.M. Rossini; L. Rosinni; F. Ferreri; , "Brain-Behavior Relations: Transcranial Magnetic Stimulation: A Review," *Engineering in Medicine and Biology Magazine, IEEE* , vol.29, no.1, pp.84-96, Jan.-Feb. 2010.
- [4] M. Chen; D.J. Mogul; , "Using Increased Structural Detail of the Cortex to Improve the Accuracy of Modeling the Effects of Transcranial Magnetic Stimulation on Neocortical Activation," *Biomedical Engineering, IEEE Transactions on* , vol.57, no.5, pp.1216-1226, May 2010.
- [5] H Osamu; I Tomonori; , "A method for estimation of stimulated brain sites based on columnar structure of cerebral cortex in transcranial magnetic stimulation," *Journal of Applied Physics* , vol.105, no.7, pp.07B303-07B303-3, Apr 2009.
- [6] Y. Katayama; K. Iramina; , "Equivalent Circuit Simulation of the Induced Artifacts Resulted From Transcranial Magnetic Stimulation on Human Electroencephalography," *Magnetics, IEEE Transactions on* , vol.45, no.10, pp.4833-4836, Oct. 2009.
- [7] I. Masakuni; K. Yohei; H. Akira; H.Takehito; U. Shoogo; I. Keiji; , "Measurements of evoked electroencephalograph by transcranial magnetic stimulation applied to motor cortex and posterior parietal cortex," *Journal of Applied Physics* , vol.105, no.7, pp.07B321-07B321-3, Apr 2009.
- [8] L. Mai; U. Shoogo; , "Calculating the electric field in real human head by transcranial magnetic stimulation with shield

- plate," *Journal of Applied Physics* , vol.105, no.7, pp.07B322-07B322-3, Apr 2009.
- [9] I. Keiji; G. Sheng; H. Akira; H. Takehito; U. Shoogo; , "Disturbance of visual search by stimulating to posterior parietal cortex in the brain using transcranial magnetic stimulation," *Journal of Applied Physics* , vol.105, no.7, pp.07B302-07B302-3, Apr 2009.
- [10] N. Kazuhisa; G. Sheng; K. Yoshinori; U. Shoogo; I. Keiji; , "Effect of the stimulus frequency and pulse number of repetitive transcranial magnetic stimulation on the inter-reversal time of perceptual reversal on the right superior parietal lobule," *Journal of Applied Physics* , vol.107, no.9, pp.09B320-09B320-3, May 2010.
- [11] A. Matsunaga; K. Nojima; M. Iwahashi; Y. Katayama; K. Iramina; , "The effect of TMS to supramarginal gyrus on event-related potential P300," *TENCON 2010 - 2010 IEEE Region 10 Conference* , vol., no., pp.1757-1760, 21-24 Nov. 2010.
- [12] A.V. Peterchev; D.L. Murphy; S.H. Lisanby; , "Repetitive transcranial magnetic stimulator with controllable pulse parameters (cTMS)," *Engineering in Medicine and Biology Society (EMBC), 2010 Annual International Conference of the IEEE* , vol., no., pp.2922-2926, Aug. 31 2010-Sept. 4 2010.
- [13] L. Mai; U. Shoogo; , "Dosimetry of typical transcranial magnetic stimulation devices," *Journal of Applied Physics* , vol.107, no.9, pp.09B316-09B316-3, May 2010.
- [14] E. Basham; Z. Yang; W. Liu; , "Circuit and Coil Design for In-Vitro Magnetic Neural Stimulation Systems," *Biomedical Circuits and Systems, IEEE Transactions on* , vol.3, no.5, pp.321-331, Oct. 2009.
- [15] A.V. Peterchev; R. Jalinous; S.H. Lisanby; , "A Transcranial Magnetic Stimulator Inducing Near-Rectangular Pulses With Controllable Pulse Width (cTMS)," *Biomedical Engineering, IEEE Transactions on* , vol.55, no.1, pp.257-266, Jan. 2008.
- [16] S. Tsuyama; Y. Katayama; A. Hyodo; T. Hayami; S. Ueno; K. Iramina; , "Effects of Coil Parameters on the Stimulated Area by Transcranial Magnetic Stimulation," *Magnetics, IEEE Transactions on* , vol.45, no.10, pp.4845-4848, Oct. 2009.
- [17] S. Yang; G. Xu; L. Wang; Y. Geng; H. Yu; Q. Yang; , "Circular Coil Array Model for Transcranial Magnetic Stimulation," *Applied Superconductivity, IEEE Transactions on* , vol.20, no.3, pp.829-833, June 2010.
- [18] S.L. Ho; G. Xu; W.N. Fu; Q. Yang; H. Hou; W. Yan; , "Optimization of Array Magnetic Coil Design for Functional Magnetic Stimulation Based on Improved Genetic Algorithm," *Magnetics, IEEE Transactions on* , vol.45, no.10, pp.4849-4852, Oct. 2009.
- [19] S. Yang; G. Xu; L. Wang; Y. Geng; H. Yu; Q. Yang; , "Circular Coil Array Model for Transcranial Magnetic Stimulation," *Applied Superconductivity, IEEE Transactions on* , vol.20, no.3, pp.829-833, June 2010.
- [20] Q. Ai; J. Li; M. Li; W. Jiang; B. Wang; , "A new transcranial magnetic stimulation coil design to improve the focality," *Biomedical Engineering and Informatics (BMEI), 2010 3rd International Conference on* , vol.4, no., pp.1391-1395, 16-18 Oct. 2010.
- [21] M. Talebinejad; S. Musallam; , "Effects of TMS coil geometry on stimulation specificity," *Engineering in Medicine and Biology Society (EMBC), 2010 Annual International Conference of the IEEE* , vol., no., pp.1507-1510, Aug. 31 2010-Sept. 4 2010.
- [22] X. Nan; C.R. Sullivan; , "An Equivalent Complex Permeability Model for Litz-Wire Windings," *Industry Applications, IEEE Transactions on* , vol.45, no.2, pp.854-860, March-April 2009.
- [23] X.Tang; C.R. Sullivan; , "Optimization of stranded-wire windings and comparison with litz wire on the basis of cost and loss," *Power Electronics Specialists Conference, 2004. PESC 04. 2004 IEEE 35th Annual* , vol.2, no., pp. 854- 860 Vol.2, 20-25 June 2004.
- [24] I.R. Walker; , "Removal of enamel from ultrafine monofilamentary wires," *Review of Scientific Instruments* , vol.75, no.5, pp.1169-1174, May 2004.
- [25] M. El-Hawary; *Principles of Electric Machines with Power Electronic Applications*. pp. 496, 2002.